Modified Stability Functions with Shear Effects for Non-Prismatic Members in Steel Plane Frames

Dr. Omar Al-Farouk Al-Damluji,
Assistant Professor,
Department of Civil Engineering,
University of Baghdad, Iraq.

Dr. Sabeeh Zaki AL-Sarraf,
Professor,
Department of Building and Construction,
University of Technology, Iraq.

Wisam Victor Yossif,
Formally Postgraduate Student,
Department of Civil Engineering,
University of Baghdad, Iraq.

ABSTRACT

The mathematical model of the tapered struts subjected to axial load is solved to obtain the modified stability functions due to shear effect as well as bending effects. The stability functions are derived for a wide range of non-prismatic struts then compared in graphical curves with stability functions excluding shear effects.

The stability functions for non-prismatic members under compressive and tensile axial loads are developed for the purpose of expressing both effects of bending and shear in a beam-column stiffness at any value of axial force under the buckling limit.

الخلاصة

لقد تم حل نموذج رياضي لعتبات لا موشورية معرضة لثقل محوري للحصول على دوال استقرارية معدلة ناتجة عن تاثيرات القص اضافة الى تاثيرات الانحناء المعهودة. لقد تم اشتقاق دوال الاستقرارية لمدى واسع من العتبات اللاموشورية ومن ثم تمت المقارنة بمنحنيات مرتسمية مع دوال الاستقرارية من دون تاثيرات القص.

لقد تم تطوير دوال الاستقرارية للاعضاء اللاموشورية تحت اثقال انضغاط و شد محورية في سبيل التعبير عن تاثيري الانحناء و القص في جساءة العتبة-العمود تحت اية قيمة من قوة محورية اقل من حد الانبعاج.

KEYWORDS
Modified Stability Functions – Shear Effects – Non-Prismatic Members –   Beam-Column
         Stiffness

INTRODUCTION

Shear effects on the elastic stability analysis are usually not considered in the analysis and design of frames made up of structural members of solid sections; this is because the distortion caused by shear is relatively small except for short members. But in different member's length and cross sectional shapes, the contribution of shear deformation to the total deflection may be appreciable. Few research works had covered shear effects in the non-

prismatic members loaded axially. Most of the researchers used approximate methods for including this effect such as a method proposed by Al-Quraishi [1] which used approximate stability functions for non-prismatic members by developing the approximate formula similarly to that derived by S. Al-Sarraf[3]. Other researchers such as AL-Fadul[2] obtained the exact stability functions for special shape of non-prismatic members and used the finite difference method to obtain the approximate stability functions for other shapes.

In the present study, a new method is adopted based on the exact stability functions including bending effects. The new expression of stability functions is derived herein by adding the effect of shear to the slope of deflection curve and to the member curvature.

Mathematical Model

When the beam-column member is loaded with a constant axial force Q, the initially straight longitudinal axis is deformed into a curve called the deflection curve which is produced by the combined effects of bending and shear deformations.

The ratio of change in slope caused by shear to that caused by moment is defined as the *shear flexibility parameter* as given by Equation (1) for prismatic members [3, 4, 5], Equation (2) for batten lacing prismatic members [1, 6] and Equation (3) for non-prismatic members [1]. The modified stability functions for beam-columns having any solid cross-sectional shapes, built-up structural members are developed in terms of the shear flexibility parameter.

$$\mu = \frac{Q_E}{GA_V} \tag{1}$$

$$\mu = Q_E \cdot \left(\frac{l_v \cdot l_h}{12EI_b} + \frac{l_v{}^2}{24EI_b} + \frac{n.l_v}{l_h.GA_b} \right) \tag{2}$$

$$\mu_2 = \frac{Q_{E2}}{GA_{V2}} \tag{3}$$

where

$Q_E = \dfrac{\pi^2 EI}{L^2}$: Euler load for prismatic members,or

$Q_E = \dfrac{\pi^2 EI_c}{L^2}$: Euler load for batten prismatic members,

$Q_{E2} = \dfrac{\pi^2 EI_2}{L^2}$: Euler load for tapered members at end 2,

EI, GA_v : flexural and shear rigidities of prismatic members ,

EI_b, GA_b : flexural and shear rigidities of batten prismatic members ,

EI_2, GA_{v2} : flexural and shear rigidities of tapered members at end 2,

I_c : moment of inertia for the vertical plate,

A_v : effective shear area for prismatic members,

A_b : cross sectional area for batten,

A_{v2} : effective shear area for tapered members at end 2,

n : numerical factor equal to 1.2 in the case of a rectangular cross section[7],

l_h : length of the batten center to center of the vertical plate, and

l_v : center to center vertical distance between two batten lacing.

PROPOSED MODIFIED STABILITY FUNCTION FOR NON-PRISMATIC MEMBERS:

A member may have a linear taper in either one or the other direction as shown in Figure (1), M_1 and M_2 are the applied end moments, a is the distance of end 2 from the origin O and b is the distance of end 1 from the origin O of zero depth. Therefore, the depth d(x) may be expressed by Equation (4):

$$d(x) = d_2(x/a) \tag{4}$$

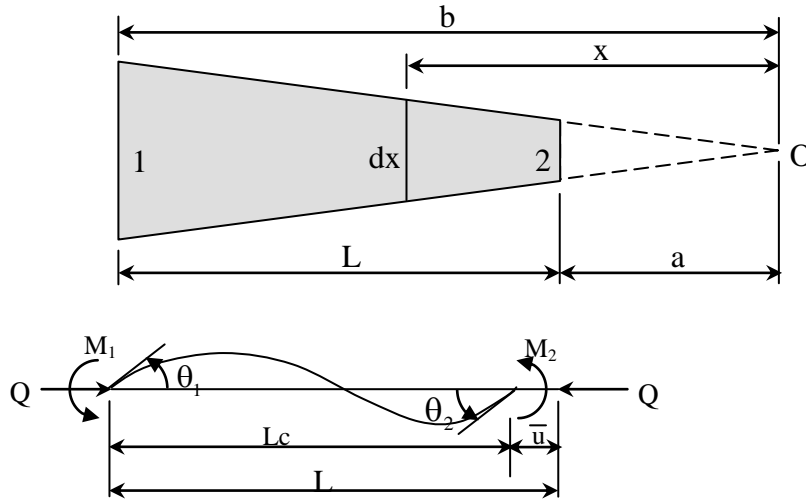where

d_1, d_2 : depths of member at ends 1and 2, respectively,

$d(x)$: depth of member at variable (x) from origin (O).

The moment of inertia of the member about the axis of bending is expressed in the form:

$$I(x) = I_2(x/a)^m \tag{5}$$

where $I(x)$ is the moment of inertia at distance x from the origin O, m is the shape factor that depends on the cross-sectional shape as given in Table (1).

Fig (1): Non-prismatic beam-column element

The effect of shear force of the non-prismatic beam-column is derived starting from the slope of the deflection curve [10]:

$$\frac{dy}{dx} = \frac{dy_b}{dx} + \frac{V(x)}{Av(x).G} \tag{6}$$

$$\frac{d^2y}{dx^2} = -\frac{M(x)}{EI(x)} + \frac{d}{dx}\left(\frac{V(x)}{Av(x).G}\right) \tag{7}$$

The bending moment and the shear force at distance x from the origin are: -

$$M(x) = \left(\frac{a-x}{L}\right)M_1 + \left(\frac{b-x}{L}\right)M_2 \mp Q(y_b + y_s) \tag{8}$$

$$V(x) = -\left(\frac{M_1 + M_2}{L}\right) + \left(Q\frac{dy_b}{dx} + Q\frac{dy_s}{dx}\right) \tag{9}$$

By substituting Equation (9) into the slope due to shear yields: -

$$\frac{dy_s}{dx} = \frac{1}{Av(x).G}.\left[-\left(\frac{M_1 + M_2}{L}\right) + Q\frac{dy_s}{dx}\right] \tag{10}$$

The effective area under shear stress at distance (x) from the origin is: -

$$Av(x) = Av_2\left(\frac{x}{a}\right)^n \tag{11}$$

The shear flexibility parameter and non-dimensional axial force parameter can be defined by the equation below:

$$\frac{Q}{Av_2.G} = \mu_2.\rho_2 \tag{12}$$

The curvature equation due to shear is derived below: -

$$\frac{d^2y_s}{dx^2} - n.\left(\frac{M_1 + M_2}{L}\right).\frac{a^n}{x}.\frac{1}{\left(1 - \mu_2.\rho_2.\frac{a^n}{x^n}\right)^2}.\frac{\mu_2.\rho_2}{Q} = 0 \tag{13}$$

MODIFIED STABILITY FUNCTIONS FOR BEAM-COLUMN WITH SQUARE CROSS SECTIONS

The basic differential equation when the shape factor n = 2 is [10]:

$$\frac{d^2y_s}{dx^2} - 2.\left(\frac{M_1 + M_2}{L}\right).\frac{a^2}{x}.\frac{1.}{\left(1 - \mu_2.\rho_2.\frac{a^2}{x^2}\right)^2}.\frac{\mu_2.\rho_2}{Q} = 0 \tag{14}$$

The solution of the second order differential equation is: -

$$y_s = \left(\frac{M_1 + M_2}{L}\right).\frac{\sqrt{\mu_2.\rho_2.a^2}}{Q}.a\tanh\left(\frac{x}{\sqrt{\mu_2.\rho_2.a^2}}\right) + C1.x + C2 \tag{15}$$

where C1 and C2 are constants of integration obtained by substituting the boundary conditions:

y = 0 at x = a and x = b yields:

$$C1 = \left(\frac{M_1 + M_2}{L}\right).\frac{\sqrt{\mu_2.\rho_2.a^2}}{Q}.\frac{a\tanh\left(\dfrac{a}{\sqrt{\mu_2.\rho_2.a^2}}\right) - a\tanh\left(\dfrac{b}{\sqrt{\mu_2.\rho_2.a^2}}\right)}{L} \tag{16}$$

$$C2 = \pm\left(\frac{M_1 + M_2}{L}\right).\frac{\sqrt{\mu_2.\rho_2.a^2}}{Q}.\frac{a\tanh\left(\dfrac{b}{\sqrt{\mu_2.\rho_2.a^2}}\right).a - a\tanh\left(\dfrac{a}{\sqrt{\mu_2.\rho_2.a^2}}\right).b}{L} \tag{17}$$

The slope of the deflection curve due to shear only is: -

$$\frac{dy_s}{dx} = -\left(\frac{M_1 + M_2}{L}\right).\frac{a^n}{x^n}.\left(1 \pm \mu_2.\rho_2.\frac{a^2}{x^2}\right)^{-1}.\frac{\mu_2.\rho_2}{Q} + C1 \tag{18}$$

The curvature of the deflected curve due to bending only is: -

$$\frac{d^2y_b}{dx^2} = -\frac{M(x)}{EI(x)} \tag{19}$$

$$I(x) = I_2\left(\frac{x}{a}\right)^m \tag{20}$$

By substituting Equation (8) and (20) into Equation (19), yields: -

$$EI_2 \left(\frac{x}{a}\right)^4 \frac{d^2 y_b}{dx^2} + Qy_b = \frac{M_1}{L}(x-a) + \frac{M_2}{L}(x-b) \tag{21}$$

where $\omega^2 = \left[Qa^4/EI_2\right]^{0.5}$.

The solution of Equation (21) and its first derivative are:

$$y_b = \sqrt{x}\left[AJ_{1/2}\left(\frac{\omega}{x}\right) + BJ_{-1/2}\left(\frac{\omega}{x}\right)\right] + \frac{M_1}{QL}(x-a) + \frac{M_2}{QL}(x-b) \tag{22}$$

$$\frac{dy_b}{dx} = A\left(\frac{\omega}{x^{1.5}}\right)J_{\frac{3}{2}}\left(\frac{\omega}{x}\right) - B\left(\frac{\omega}{x^{1.5}}\right)J_{-\frac{3}{2}}\left(\frac{\omega}{x}\right) + \frac{M_1 + M_2}{QL} \tag{23}$$

where the boundary conditions are:

at   x = a,   y = 0, and dy/dx = θ_{2b},

and   at   x = b,   y = 0, and dy/dx = θ_{1b}.

The values of the constants A and B are obtained by substituting the boundary conditions into Equation (22).

$$A = \frac{M_1 J_{-\frac{1}{2}}(\alpha)\sqrt{a} + M_2 J_{-\frac{1}{2}}(\beta)\sqrt{b}}{\sqrt{a}\sqrt{b}\,ZQ}$$

$$B = -\frac{M_1 J_{\frac{1}{2}}(\alpha)\sqrt{a} + M_2 J_{\frac{1}{2}}(\beta)\sqrt{b}}{\sqrt{a}\sqrt{b}\,ZQ}$$

where

$$Z = J_{\frac{1}{2}}(\alpha)J_{-\frac{1}{2}}(\beta) - J_{-\frac{1}{2}}(\alpha)J_{\frac{1}{2}}(\beta)$$

$$\alpha = \frac{\omega}{a} \;,\; \beta = \frac{\omega}{b} \;,\; \rho_2 = \frac{QL^2}{EI_2\pi^2} \;,\; \omega = \left(\frac{a^4 Q}{EI_2}\right)^{0.5}$$

Therefore, the total slope of the deflected curve which is $\frac{dy}{dx} = \frac{dy_b}{dx} + \frac{dy_s}{dx}$ becomes:

$$\frac{dy}{dx} = A\left(\frac{\omega}{x^{1.5}}\right)J_{\frac{3}{2}}\left(\frac{\omega}{x}\right) - B\left(\frac{\omega}{x^{1.5}}\right)J_{-\frac{3}{2}}\left(\frac{\omega}{x}\right) + \frac{M_1 + M_2}{QL} - \left(\frac{M_1 + M_2}{L}\right)\cdot\frac{a^2}{x^2}\cdot\frac{1}{\left(1-\mu_2.\rho_2.\frac{a^2}{x^2}\right)}\cdot\frac{\mu_2.\rho_2}{Q} + C1 \tag{24}$$

The boundary conditions of $\frac{dy}{dx}$ at x = a and at x = b are:

$$\frac{dy}{dx} = \frac{\theta_{1b} - \frac{\mu_2.\rho_2}{Q.u^2}\left(\frac{M_1+M_2}{L}\right)}{1 - \frac{\mu_2.\rho_2}{u^2}} \qquad \text{at x = b} \tag{25}$$

$$\frac{dy}{dx} = \frac{\theta_{2b} - \frac{\mu_2.\rho_2}{Q}\left(\frac{M_1+M_2}{L}\right)}{1 - \mu_2.\rho_2} \qquad \text{at x = a,} \tag{26}$$

By substituting the above boundary conditions in Equation (24), then:

$$\left(A\left(\frac{\omega}{b^{1.5}}\right)J_{\frac{3}{2}}\left(\frac{\omega}{b}\right)-B\left(\frac{\omega}{b^{1.5}}\right)J_{-\frac{3}{2}}\left(\frac{\omega}{b}\right)+\frac{M_1+M_2}{Q.L}-\left(\frac{M_1+M_2}{Q.L}\right)\cdot\frac{\mu_2.\rho_2}{u^2-\mu_2.\rho_2}+C1\right)\cdot\left(1-\frac{\mu_2.\rho_2}{u^2}\right)$$

$$+\frac{\mu_2.\rho_2}{Q.u^2}\left(\frac{M_1+M_2}{L}\right)=\theta_{1b} \qquad \text{at } x=b \qquad (27)$$

$$\left(A\left(\frac{\omega}{a^{1.5}}\right)J_{\frac{3}{2}}\left(\frac{\omega}{a}\right)-B\left(\frac{\omega}{a^{1.5}}\right)J_{-\frac{3}{2}}\left(\frac{\omega}{a}\right)+\frac{M_1+M_2}{Q.L}-\left(\frac{M_1+M_2}{Q.L}\right)\cdot\frac{\mu_2.\rho_2}{1-\mu_2.\rho_2}+C1\right)\cdot(1-\mu_2.\rho_2)$$

$$+\frac{\mu_2.\rho_2}{Q}\left(\frac{M_1+M_2}{L}\right)=\theta_{2b} \qquad \text{at } x=a \qquad (28)$$

Thus the stability functions are:

$$S_1=\frac{Z_1}{EI_2}\frac{K_a\left(D_1QL+B_1QL+1\right)+\mu_2.\rho_2}{Q} \qquad (29)$$

$$SC=\frac{Z_1}{EI_2}\frac{K_bu^2\left(C_1QL+A_2QL+1\right)+\mu_2.\rho_2}{Qu^2} \qquad (30)$$

$$S_2=\frac{Z_1}{EI_2}\frac{K_bu^2\left(A_1QL+A_2QL+1\right)+\mu_2.\rho_2}{Q.u^2} \qquad (31)$$

where the symbols A1, B1, C1, D1, A2, B2, Ka, Kb and Z are given in Appendix

The modified stability functions for beam-column with a rectangular cross section bent about the major axis and a rectangular cross section bent about the minor axis are listed in the Appendix:

Experimental Determination of the Elastic Critical Load:
It is based on the fact that the stiffness of a structure decreases with the increase of the axial force in the members. At the critical load, the stiffness of the structure is zero. Thus, it is possible to determine the elastic critical load of structures by expressing the stiffness as described below.

The natural frequency of oscillation of a frame decreases with the increase of the applied external load. When the vibration stiffness is plotted against the applied load, an almost linear relationship is obtained. An estimation of the elastic critical load is made by the extrapolation of the linear part of the graph. In frames with complicated sways, experimental determination of the elastic critical load is obtained by dynamic stiffness plots.

In general, for any system, the frequency of vibration may be calculated as in the following [8]: -

$$f=\frac{1}{2\pi}\sqrt{\frac{k}{\frac{\Sigma W}{g}}} \qquad (32)$$

where

  f   : frequency in cycle/sec,
  k   : stiffness of structure,
  W   : summation of external load on frame, and
  g   : acceleration due to gravity.
  Equation (32) may be written as: -

$$k = \frac{(2\pi)^2}{g} \Sigma Wf^2 \quad \text{for constant g,} \tag{33}$$

$$k \propto \Sigma W.f^2$$

The stiffness of the primary buckling mode is a linear function of the applied external load. Thus, the relation between the total applied load ΣW and the parameter (ΣWf^2) is approximately linear.

This method was widely used in finding out the elastic critical load experimentally. In this test which is done in present study, the structure is subjected to push at every applied load and the number of vibrations is calculated at this time. Then, the frequency, f, is equal to the number of vibrations over the unit time for that total load.

The cantilever beam-column models are manufactured from steel materials with dimensions of high accuracy. These models consist of four different non-prismatic cross-sectional types and one prismatic type in four different cases of batten lacing. The number of sway cycles is recorded for 6 seconds for different loads at the free end, then the relation between the loads and the beam-column dynamic stiffness is drawn to obtain the elastic critical load. The results of each type of non-prismatic member that is subjected to experimental load are reported in Table (1). The same thing is used for each case of batten lacing. The model types are shown in Appendix. Table (2) to (9) expose the average recorded data for three non-prismatic models of the described properties in Table (1). In other words, each type has dimensions defined in Table (1).

Table (1) Models dimensions

Test No.	Cross-section	m	u	Length, cm	Width, mm	Depth, mm
1	Square	4	2	30	6 – 12	6 – 12
2	Rectangular	3	2	40	3	1.5 – 3
3	Rectangular	1	2	40	15 – 30	2
4	Rectangular box 1 mm thickness	2.4	2	75	1.5	7 – 14
5	2 cm Batten lacing	-	1	40	25	2mm each part
6	5 cm Batten lacing	-	1	40	25	2mm each part
7	10 cm Batten lacing	-	1	40	25	2mm each part
8	20 cm Batten lacing	-	1	40	25	2mm each part

Table (2): Average results of 3 models having shape factor m=4

Axial Force, kN	Mass Load, kg	No. of cycles	Frequency rad/6 sec
0.0004905	0.050	49	51.31268
0.0009810	0.100	32	33.51032
0.0014715	0.150	23	24.08554
0.0019620	0.200	18	18.84956
0.0024525	0.250	14	14.66077
0.0029430	0.300	11	11.51917

Table (3): Average results of 3 models having shape factor m=3

Axial Force, kN	Mass Load, kg	No. of cycles	Frequency, rad/6 sec
0.000981	0.100	155	162.3156
0.001962	0.200	109	114.1445
0.002943	0.300	89	93.20059
0.003924	0.400	76	79.58702
0.004905	0.500	68	71.20944
0.009810	1.000	47	49.21829
0.049050	5.000	16	16.75516

Table (4): Average results of 3 models having shape factor m=1

Axial Force, kN	Mass Load, kg	No. of cycles	Frequency rad/6 sec
0.000981	0.100	84	87.9645
0.001962	0.200	59	61.7846
0.002943	0.300	47	49.2182
0.003924	0.400	41	42.9350
0.004905	0.500	36	37.6990
0.009810	1.000	24	25.1327
0.049050	5.000	3	3.1415

Table (5): Average results of 3 models having shape factor m=2.4

Axial Force, kN	Mass Load kg	No. of cycles	Frequency, rad/6 sec
0.000981	0.100	292	305.7817
0.001962	0.200	206	215.7227
0.002943	0.300	168	175.9292
0.003924	0.400	146	152.8908
0.004905	0.500	130	136.1357
0.009810	1.000	92	96.34217
0.049050	5.000	40	41.8879

Table (6): Average results of 3 prismatic models with 2 cm batten lacing

Axial Force, kN	Mass Load, kg	No. of cycles	Frequency rad/6 sec
0.000981	0.100	1007	1054.528
0.001962	0.200	712	745.604
0.002943	0.300	581	608.421

0.003924	0.400	503	526.740
0.004905	0.500	450	471.238
0.009810	1.000	318	333.008
0.098100	10.00	100	104.719

Table (7): Average results of 3 prismatic models with 5 cm batten lacing

Axial Force, kN	Mass Load, kg	No. of cycles	Frequency rad/6 sec
0.000981	0.100	603	631.460
0.001962	0.200	426	446.106
0.002943	0.300	348	364.424
0.003924	0.400	301	315.206
0.004905	0.500	269	281.696
0.009810	1.000	190	198.967
0.049050	5.000	85	89.011
0.098100	10.00	60	62.831

Table (8): Average results of 3 prismatic models with 10 cm Batten lacing

Axial Force, kN	Mass Load, kg	No. of cycles	Frequency, rad/6 sec
0.000981	0.100	356	372.8023
0.001962	0.200	252	263.8938
0.002943	0.300	205	214.6755
0.003924	0.400	178	186.4012
0.004905	0.500	159	166.5044
0.009810	1.000	112	117.2861
0.049050	5.000	50	52.35988
0.098100	10.00	35	36.65191

Table (9): Average results of 3 prismatic models with 20 cm batten lacing

Axial Force, kN	Mass Load, kg	No. of cycles	Frequency, rad/6 sec
0.000981	0.100	194	203.1563
0.001962	0.200	137	143.4661
0.002943	0.300	112	117.2861
0.003924	0.400	97	101.5782
0.004905	0.500	87	91.10619
0.009810	1.000	61	63.87905
0.049050	5.000	27	28.27433
0.098100	10.00	19	19.89675

The results are obtained experimentally and theoretically. They are then compared as in the following:

Experimentally: The results are analyzed graphically to obtain the buckling load at the vanished stiffness by extending the relation between the stiffness and mass linearly. Figures (2) to (9) show the buckling load for eight different models.

Theoretically: For a cantilever tapered column having load at the top free end, the stiffness matrix is[9]:

$$k = \begin{bmatrix} S_{\Upsilon} & -(S_{\Upsilon} + SC) \\ -(S_{\Upsilon} + SC) & q \end{bmatrix}$$

where $q = S_1 + S_2 + 2SC - \pi^2 \rho_2$, $\rho_2 = \dfrac{QL^2}{EI_2 \pi^2}$

The results shown in Tables (10) and (11) present the obtained results by considering the eight different models experimentally and theoretically.
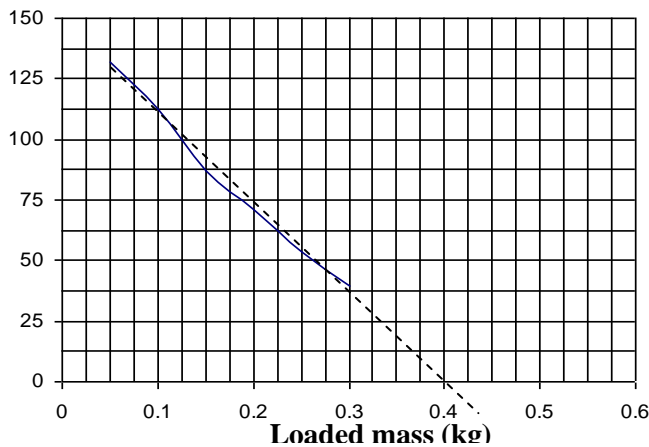
Fig (2): Stiffness-mass relation of model 1
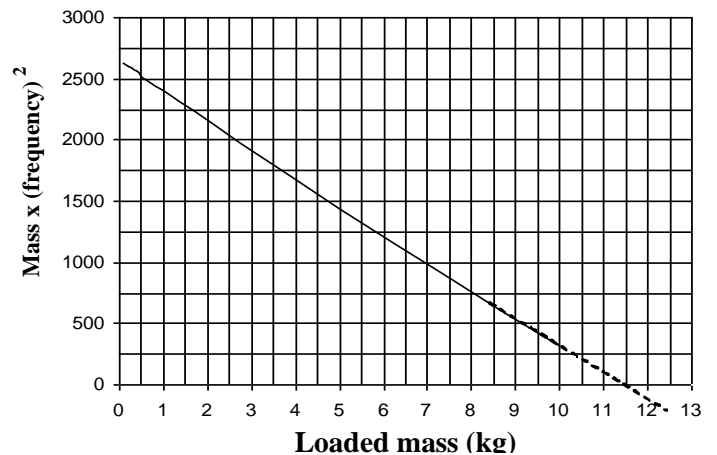
Fig (3): Stiffness-mass relation of model 2
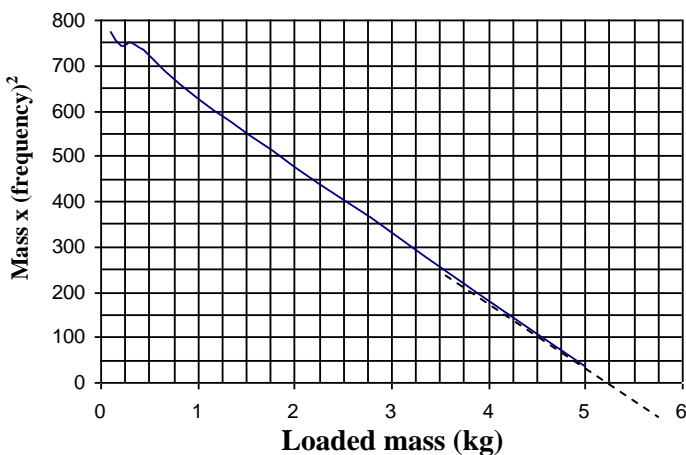
Fig (4): Stiffness-mass relation of model 3
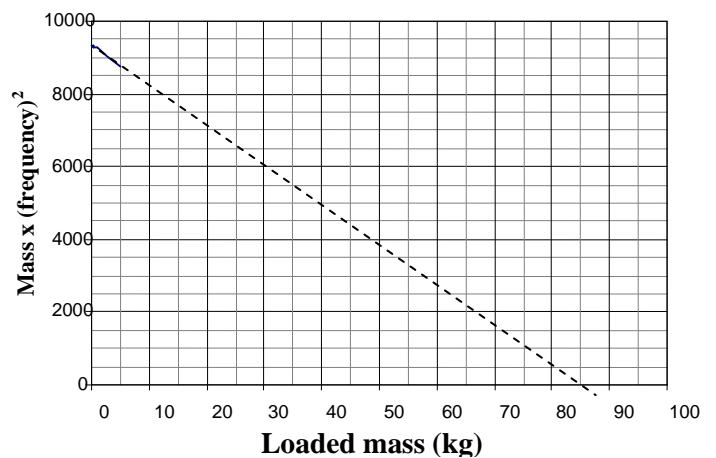
Fig (5): Stiffness-mass relation of model 4
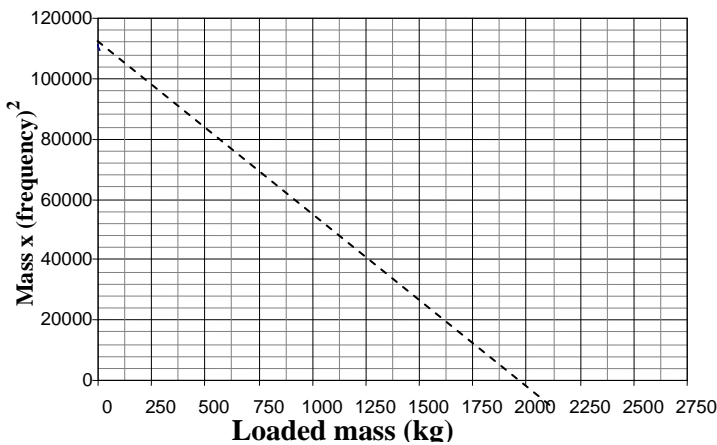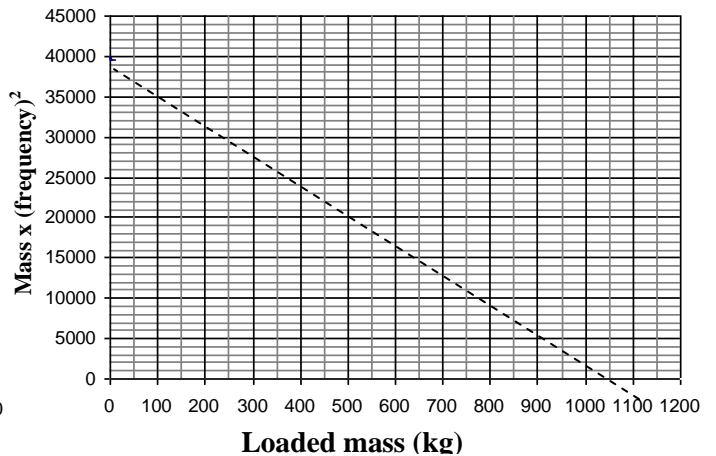
Fig (6): Stiffness-mass relation of model 5

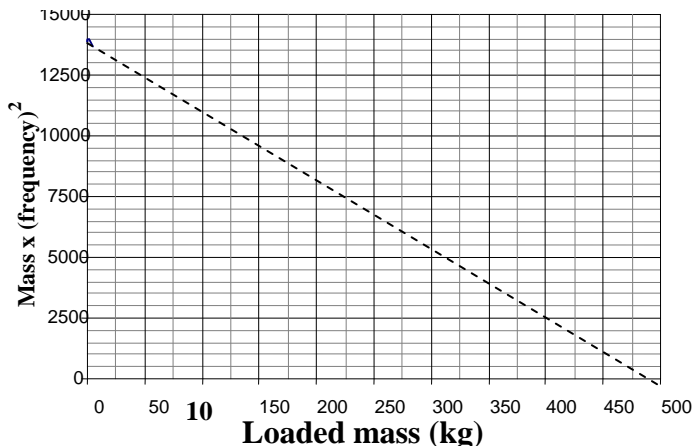**Fig (7): Stiffness-mass relation of model 6**
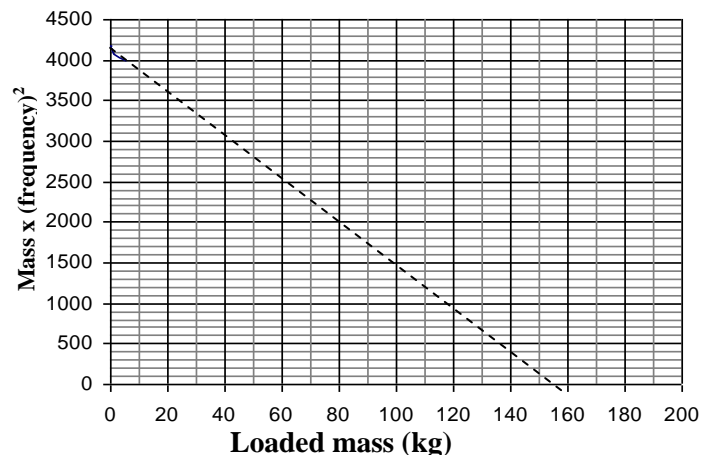

Fig (8): Stiffness-mass relation of model 7

Fig (9): Stiffness-mass relation of model 8

(10) Experimental and theoretical results of model 1, 2, 3 and 4

Test No.	Experimental results		Theoretical results			
	Q_{cr}, kN	Q_{cr}, kg	ρ_2	S_1	S_2	SC
1	0.003946	0.405	1.6659	27.31426	6.82856	8.61646
2	0.112815	11.500	1.0840	16.959	5.982	6.124
3	0.051551	5.255	0.4179	6.19183	4.38816	3.0121
4	0.847 584	86.400	0.823	12.608	5.481	4.958

Table (11) Experimental and theoretical results of model 5, 6, 7 and 8

Test No.	Experimental results		Theoretical results			
	Q_{cr}, kN	Q_{cr}, kg	ρ	μ	s	sc
5	18.474	1883	0.1841102	1.431531	1.862895	0.292099
6	10.607	1081	0.1057058	5.460222	1.175894	-0.394902
7	4.735	482	0.047188	17.19175	0.922095	-0.648701
8	1.581	152	0.015755	59.4687	0.826299	–0.744498

The buckling load is obtained for the first model divided into two, three and four non-prismatic elements. Hereafter, the stability functions and non-dimensional axial force parameter for each element are obtained and given in Table (12).

Table (4) Stability Functions for model 1 divided into 1, 2, 3 and 4 tapered members

Element	L m	Q kN	Stability Function	Values of Stability Functions			
				First	Second	Third	Fourth
One	0.3	0.00394	S_1	27.3143	-	-	-
			SC	8.61646	-	-	-
			S_2	6.82856	-	-	-
			ρ_2	1.66590	-	-	-
Two	0.15	0.00394	S_1	12.6399	9.3238336	-	-
			SC	4.63927	3.5783314	-	-
			S_2	5.61763	5.2446338	-	-
			ρ_2	0.416475	0.0822700	-	-
Three	0.01	0.00394	S_1	9.139763	7.7054150	6.8649449	-
			SC	3.613771	3.1403804	2.8841442	-
			S_2	5.141116	4.9314656	4.7673228	-
			ρ_2	0.185100	0.0585664	0.0239888	-
Four	0.075	0.00394	S_1	7.629459	6.8353036	6.3118599	5.9462715
			SC	3.155855	2.8903702	2.7254391	2.6124706
			S_2	4.882853	4.7467386	4.6372774	4.5526189
			ρ_2	0.104119	0.0426468	0.0205665	0.0111013

The experimental data for models from 1 to 8 are identical with theoretical results that used modified stability functions by including shear effect. From the previous results, the elastic critical load of models 5, 6, 7 and 8 are compared with others, as shown in Figure (10) to represent the effect of increasing the number of batten lacings on elastic critical load in a prismatic member.
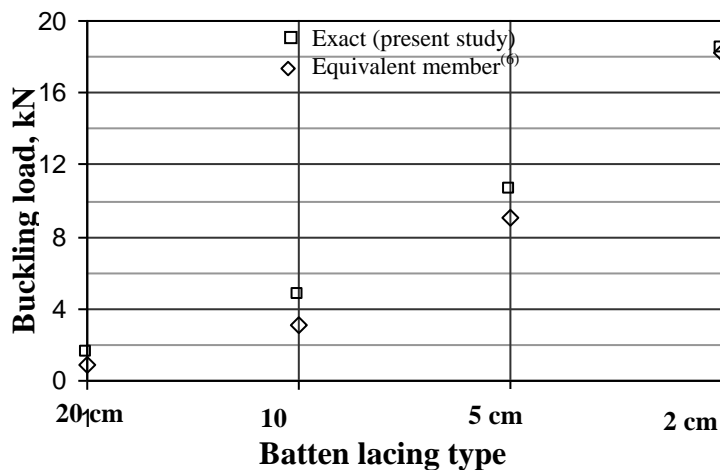
Fig (10): Buckling load on prismatic member for different batten lacings

It is found that the prismatic member having 2cm-batten lacing buckled after the three other models which have less number of battens lacing. On the other hand, the prismatic member having 20cm batten lacings buckled before the three other models which have a larger number of battens lacings. This means that, when the number of batten lacing increased, the buckling load increased. The other type of comparison is presented in Table (13) for the elastic critical load of the present study and the equivalent member [6]. It is found that the elastic critical load, which is obtained from the present study, is more than that obtained from the equivalent member. Their values are close to each other. The error percent reduces when the number of batten lacings is increased.

Table (13): Buckling load and displacement comparisons

Test	No. of batten lacings	Buckling load, kN		Ratio*	Error** %	Displacement at critical load, m	
		Present study	Equivalent member			Present study	Equivalent member
5	20	18.474	18.2631	0.9886	1.14	0.2163	0.2080
6	8	10.6066	9.03929	0.8522	14.78	0.1352	0.1315
7	4	4.735	3.10014	0.6547	34.52	0.0617	0.0512
8	2	1.5809	0.85348	0.5399	46.01	0.0272	0.0191

* The ratio between the buckling load of equivalent member to that of the present study.

** Error = Deference between the buckling load of the present study and equivalent member divided by the buckling load of the present study.

From the above experimental works and theoretical results, the stability functions are very close.

Conclusions

1. The modified stability functions including the effect of bending and shear are compared with the stability functions including the effect of bending only for the same properties of non-prismatic beam-columns under different axial forces and cross-sectional areas. These conditions give different ratios of stability functions, which include and exclude shear effect. The effect of shear is summarized in Table (14) which shows: -

**Table (14): Ratios between stability functions
excluding and including the effect of shear**

ρ_2 \ μ_2		0.00	2.00
0.0001	S_1	0.999747	0.999813
	SC	0.999600	0.999888
	S_2	0.999838	0.999998
0.0400	S_1	0.908997	0.928652
	SC	0.854400	0.958576
	S_2	0.941763	0.999844

a. The effect decreases the stability functions with increasing of non-dimensional axial force parameters in the compression range.

b. The effect increases the stability function with increasing of value of shear parameter.

c. The minimum effect is at maximum axial force and minimum shear parameter (0.0001).

d. The maximum effect is at zero axial force and maximum shear parameter (0.04).

    e. The effect of shear parameter exceeds the effect of non-dimensional axial force parameter.

2. In batten laced members, the shear flexibility parameter is decreased with increasing the number of batten lacings between two main columns. The limit of buckling load is increased by reducing the additional deformation due to shear strain as given by which summarizes the buckling load data for models 5, 6, 7 and 8.

3. .It is found that the prismatic member having 2cm batten lacing buckled after the three other models which have less number of battens lacings. On the other hand, the prismatic member having 20cm batten lacings buckled before the three other models which have a larger number of battens lacings. This means that, when the number of batten lacing is increased, the buckling load is increased.

4. It is found that the elastic critical load, which is obtained from the present study, is larger than the elastic critical load obtained from the equivalent prismatic member given by Timoshenko formula [6] .Their values are close to each other and the error percent is reduced when the number of batten lacings is increased.

REFERENCES:
1. Al-Quraishi, H. A. A., "Large Displacement Elastic Stability Analysis of Plane Frames Including Shear Effect", M.Sc. Thesis, University of Technology, Iraq, 1999.
2. Al-Fadul, M. A., "Stability Functions for Non-Prismatic Members Including Shear Effect", M. Sc. Thesis, University of Kufa, Iraq, 2005
3. Al-Sarraf, S. Z., "Shear Effect on the Elastic Stability of Frames", The Structural Engineer, June 1986, pp. 43-47.
4. Lin, F.J., Glauser, E.C., and Johnston, B.G., "Behaviour of Laced and Battened Structural Members", Journal of the Structural Division, ASCE, Vol.96, No. ST7, July 1970, pp. 1377-1401.
5. Lindgren, S., "Shear Flexibility", Journal of the Structural Division, ASCE, Vol.105 No. ST10, October 1979,Technical Note 2117-2121.
6. Timoshenko, S. and Gere, J.M., "Theory of Elastic Stability", 2nd edition, New York, McGraw Hill Book Co., Inc., 1961.
7. Al-Sarraf, S.Z., "Discussion of Frames of Solid Bars of Varying Cross Sections", Journal of the Structural Division, ASCE 81, No. ST1, February 1985, pp 318.
8. Al-Sarraf S.Z., "Elastic Stability of Frameworks", Ph.D. Thesis presented to the University of Liverpool at Liverpool, England, July, 1964.
9. Al-Sarraf, S. Z., "Elastic Instability of Frames with Uniformly Tapered Members", The Structural Engineer, March 1979, pp. 18-24.
10. Yousif, W. V., "Modified Stability Functions with Shear Effects for Non-Prismatic Members in Steel Plane Frames and Members Inside Soils", Ph.D. Thesis, Department of Civil Engineering, University of Baghdad, April 2006.

Appendix

m=3	$S_1 = \dfrac{Z_1}{EI_2} \dfrac{K_a(D_1 QL + B_1 QL + 1) + \mu_2 . \rho_2}{Q}$
	$SC = \dfrac{Z_1}{EI_2} \dfrac{K_b(C_1 QL + A_2 QL + 1) + \mu_2 . \rho_2}{Q.u}$
	$S_2 = \dfrac{Z_1}{EI_2} \dfrac{K_b . u(A_1 QL + A_2 QL + 1) + \mu_2 . \rho_2}{Q.u}$
m=1	$S_1 = \dfrac{Z_1}{EI_2} \dfrac{K_a(D_1 QL + B_1 QL + 1) + \mu_2 . \rho_2}{Q}$
	$SC = \dfrac{Z_1}{EI_2} \dfrac{K_b(C_1 QL + A_2 QL + 1) + \mu_2 . \rho_2}{Q.u}$
	$S_2 = \dfrac{Z_1}{EI_2} \dfrac{K_b . u(A_1 QL + A_2 QL + 1) + \mu_2 . \rho_2}{Q.u}$
m=2	$S_1 = \dfrac{QLb}{PEI_2}\left[L\beta\cos\psi - 0.5(b+a)\sin\psi\right]$
	$SC = \dfrac{QLab}{PEI_2}\left(\sin\psi - \dfrac{\beta L}{a^{0.5} b^{0.5}}\right)$
	$S_2 = \dfrac{QLa}{PEI_2}\left(\beta L\cos\psi - 0.5(a+b)\sin\psi\right)$
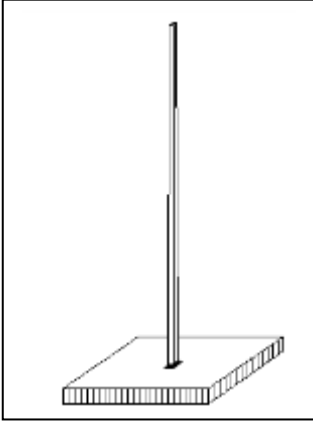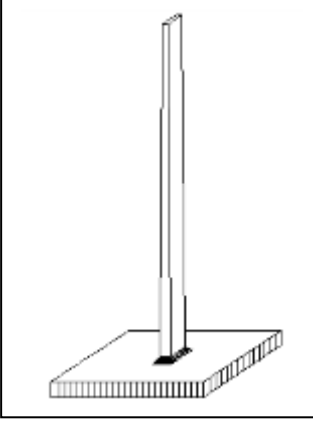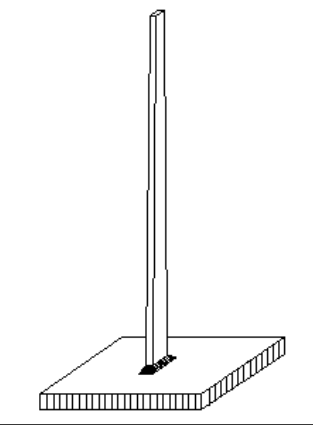
m=4	$Z_1 = L / [K_a \dfrac{\mu_2 . \rho_2}{Q.u^2}(D_1 - B_1) - K_b K_a L\left(A_2(B_1 - D_1) + C_1 B_1 + B_2(C_1 - A_1) + \dfrac{C_1 - D_1}{QL} + \dfrac{B_1 - A_1}{QL} - A_1 D_1\right)$ $- K_b \dfrac{\mu_2 . \rho_2}{Q}(C_1 - A_1)]$
m=3	$Z_1 = L / [K_a \dfrac{\mu_2 . \rho_2}{Q.u}(D_1 - B_1) - K_b K_a L\left(A_2(B_1 - D_1) + C_1 B_1 + B_2(C_1 - A_1) + \dfrac{C_1 - D_1}{QL} + \dfrac{B_1 - A_1}{QL} - A_1 D_1\right)$ $- K_b \dfrac{\mu_2 . \rho_2}{Q}(C_1 - A_1)]$
m=1	$Z_1 = L / [K_a \dfrac{\mu_2 . \rho_2}{Q.u}(D_1 - B_1) - K_b K_a L\left(A_2(B_1 - D_1) + C_1 B_1 + B_2(C_1 - A_1) + \dfrac{C_1 - D_1}{QL} + \dfrac{B_1 - A_1}{QL} - A_1 D_1\right)$ $- K_b \dfrac{\mu_2 . \rho_2}{Q}(C_1 - A_1)]$

m=2	$A = -\dfrac{M_1 + M_2 u^{0.5}\cos\psi}{Q u^{0.5}\sin\psi}$
	$B = M_2 / Q$

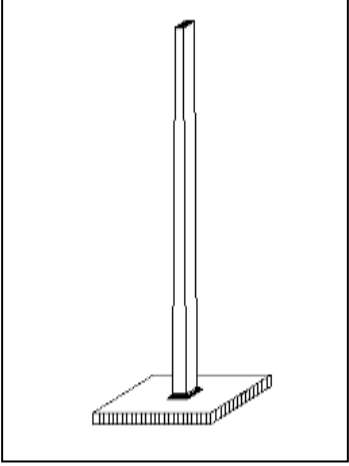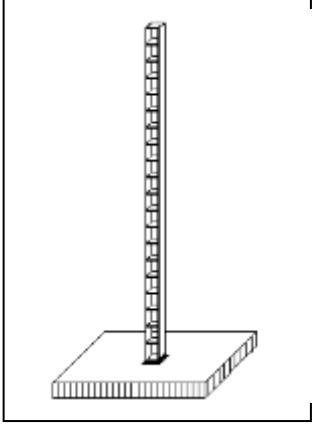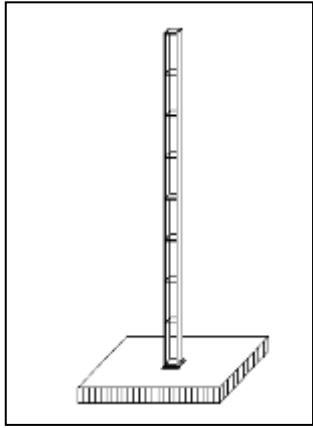$$\beta = \sqrt{\frac{\overline{\rho}_2 \pi^2}{(u-1)^2} - 0.25}$$

$$\psi = \beta \ln\left(\frac{b}{a}\right)$$

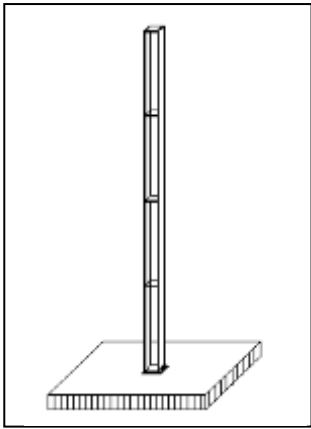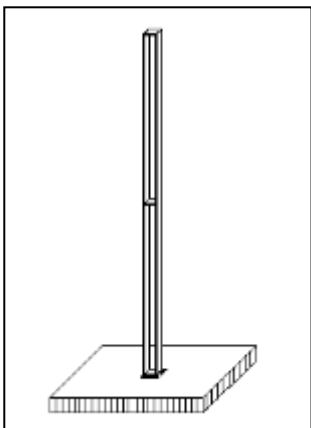$$P = L(\beta^2 - 0.25)\sin\psi + (a+b)\beta\cos\psi - 2\beta a^{0.5}b^{0.5}$$

Model 1		
Model 2		
Model 3		

Model 4		
Model 5		
Model 6		

Model 7		
Model 8		

List of symbols

Symbol	Symbol Definition
A_v	Effective shear area for prismatic members
A_b	Cross sectional area for batten
A_{v2}	Effective shear area for tapered members at end 2
E	Modulus of elasticity
I_2	Moment of inertia for tapered member at end 2
$I(x)$	Moment of inertia at distance x from the origin O for tapered member
I_c	Moment of inertia for vertical plate
I_h	Length of the batten center to center of vertical plate
I_v	Center to center vertical distance between two battens lacing
M_1, M_2	Applied moment at end 1 and 2 respectively
$M(x)$	Bending moment at distance x from the origin O
Q	Constant axial force
Q_E	Euler load ($\pi^2 EI / L^2$)
S_1	Flexural stiffness factor for tapered member at end 1
S_2	Flexural stiffness factor for tapered member at end 2
SC	Flexural carry-over factor for tapered member

V	Shear force
a	Distance of end 2 from the origin O for tapered member
b	Distance of end 1 from the origin O for tapered member
d_1, d_2	Depth of tapered member at end 1 and 2 respectivily
$d(x)$	Depth of tapered member at distance x fro origin O
f	Frequency in cycle /sec
g	Acceleration due to gravity
k	Stiffness of structure
m	Shape factor
n	Numerical factor equal to 1.2 in the case of a rectangular cross section
u	Tapering ratio
W	Summation of external load on frame
y	Lateral deflection at distance x along the member
μ	Shear flexibility parameter
θ_1, θ_2	End rotations at end 1 and 2
ρ_2	Non-dimensional axial force parameters for tapered member